ELSEVIER

Journal of Photochemistry and Photobiology
A: Chemistry 88 (1995) 153–162

Journal of PHOTOCHEMISTRY AND PHOTOBIOLOGY A:CHEMISTRY

Solubilization of a 3*H*-indole molecular probe in surfactant micelles and vesicles: a spectral and photophysical study

Ranjit S. Sarpal [1], Michel Belletête, Gilles Durocher *

Département de Chimie, Université de Montréal, C.P. 6128, Succ. A, Montréal, Qué. H3C 3J7, Canada

Received 8 November 1994; accepted 10 January 1995

Abstract

An absorption and fluorescence spectral study on the solubilization behavior of 2-[(*p*-methylamino)phenyl]-3,3-dimethyl-5-carboethoxy-3*H*-indole (**I**) in sodiumdodecyl sulfate (SDS), cetyltrimethylammonium bromide (CTAB) aqueous micelles and dioctadecyldimethylammonium bromide (DODAB) surfactant vesicles has been carried out. Using spectral correlations with the polarity parameters, polarity values corresponding to a dielectric constant *D* of 48, 33 and 36 have been estimated for SDS, CTAB and DODAB respectively at 298 K. The nature of the binding site has been discussed. In DODAB vesicles, the probe moves in average toward the center of the bilayer as a function of temperature. This behavior of molecule **I** in DODAB has been effectively used to discuss its permeability to external solubilizates. Fluorescence decay time analysis has been used to discuss the molecular recognition in these surfactant assemblies. pH effects on the ring nitrogen protonation (neutral–monocation equilibrium) have been carried out and the extent of monocation formation has been discussed on the basis of the charge nature of surfactant organized assemblies.

Keywords: Solubilization; 3H-Indole; Micelles; Vesicles

1. Introduction

The membrane mimetic systems provide elegant alternatives to the complex biological membranes [1,2]. Although no single model system is likely to duplicate all the excellent structural and functional features of natural membranes, the studies in such synthetic microstructures can serve to identify concepts and mechanisms likely to be useful in a biological context [3,4].

The surfactant amphiphiles in solution can form a variety of aggregates, whose molecular architecture depends on the surfactant amphiphiles and the experimental conditions used [1]. Single chain surfactants form micelles [5,6], whereas surfactant molecules equipped with two long alkyl chains tend to form bilayer vesicles [4,7–9]. Over the past few decades, a considerable amount of research activity has been exercised toward these microstructures and the researchers have approached the domain of membrane mimetic chemistry with diverse interests, e.g. energy storage, drug encapsulation, novel reaction media etc. [10–17]. Diverse interests in such microreactors have always prompted the scientists to characterize them from both structural and dynamic points of view [17–26].

3*H*-indole molecules are sensitive to the environments [27–31], thus qualifying to act as potential probe candidates for the microstructures [6]. The motivation behind this work thus involves a long-range project designed to use 3*H*-indoles as molecular probes to the synthetic microreactors initially and then to tissues and cells at a later stage. In this respect, it is known that the applications of fluorescence to clinical chemistry and imaging are not limited by the instrument technology, but rather by the available probes that display specific analyte sensitivity [32]. Over the past few years, we have successfully been able to identify the usefulness of these 3*H*-indole molecular probes in characterizing mean structural properties of reverse micelles [33], aqueous micelles [34,35] and surfactant vesicles [36]. Here, we report the solubilization behavior of 2-[(*p*-methylamino)phenyl]-3,3-dimethyl-5-carboethoxy-3*H*-indole (**I**) (Scheme 1) in sodiumdodecyl sulfate (SDS), cetyltrimethylammonium bromide (CTAB) aqueous micelles and dioctadecyldimethylammonium bromide (DODAB) surfactant vesicles. Molecule **I** has already been studied in some homogeneous solvents [29], and some more detailed studies in homogeneous environments will be reported in this paper. The detailed

[1] Present address: Department of Chemistry, Washington State University, Pullmann, WA 99164, USA.

* Corresponding author.

SSDI 1010-6030(95)04036-6

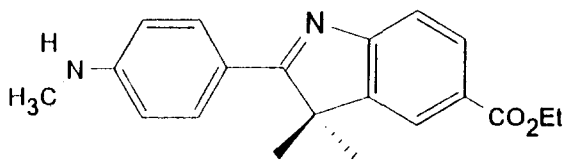

Scheme 1.

mechanism behind the spectral properties and behavior of this probe in homogeneous media being now well known and understood; the present study shows that, as well as polarity, hydrogen bonding complexes also play a role at the binding site of molecule I in organized assemblies. Also, pH studies reveal that the extent of the formation of monocation species as a function of pH depends on the charge nature of the surfactant assemblies.

2. Experimental section

Synthesis and purification of molecule I were done according to modified methods of Skrabal et al. [37] and were reported in the M.Sc. thesis of Popowycz [38]. Analytical grade reagent sodium hydroxide, sulfuric acid, hydrochloric acid and methanol were used as received. Sephadex G-50 "fine" obtained from Sigma was used without purification. Surfactants SDS (Aldrich, 98%) and CTAB (Aldrich) were purified according to the method reported recently [34]. DODAB was received from Eastman Kodak and was purified in an 90:10 acetone–water mixture. All the surfactants after purification were stored in a desiccator. Concentrations of CTAB and SDS used in all measurements were 0.01 M and 0.06 M respectively, whereas the concentration of molecule I was between 1×10^{-6} and 2×10^{-6} M.

The preparation of DODAB vesicles was as follows: an aliquot of 10^{-3} M solution of molecule I in methanol was added to methanol solution of DODAB (18 mg) in a vial. This mixture was mixed by slight shaking and was dried in a vacuum desiccator. A thin film was formed along the sides of the vial. To this, 2 ml of aqueous solution having pH ≈ 8 was added. This solution was sonicated on a probe type sonicator (Fisher 300) set at 50 W with a relative output of 70%, at 70 °C for 10 min. The solution was cooled down to room temperature and was transferred into Eppendorf standard micro test tubes. This was centrifuged on a megafuge supplied by Baxter products (model 2630) at 3000 rev min^{-1} for 15 min. This helps to homogenize the vesicles and, in addition, it removes titanium particles released by the tip of the sonicator. A measured amount of this solution was passed through a Sephadex column (15 cm × 1.5 cm). Fractions of equal volume were collected in glass vials and the presence of vesicles with solubilized probes was monitored by UV spectrophotometry. All the fractions obtained from the column containing vesicles were mixed together. The dilution of vesicles was 3–4 times. Since DODAB vesicles exhibit absorbance between 250 nm and 400 nm, vesicles without molecule I were prepared in a similar fashion as mentioned above, in order to use them in the reference compartment of the UV spectrophotometer. On the contrary, DODAB vesicles did not exhibit any spurious emission. The pH in micellar solutions was adjusted using sodium hydroxide and sulfuric acid. In order to vary the pH of solutions in vesicles, hydrochloric acid was used instead of sulfuric acid because, at pH values below 3, DODAB solutions precipitate in sulfuric acid. To maintain the same pH in the inner pool and on the surface of DODAB, all pH solutions were "freeze thawed" five times and the solutions were resonicated.

The absorption spectra were recorded on a Philips PU-8800 UV-visible spectrophotometer. Corrected fluorescence spectra were measured on a Spex Fluorolog-2 spectrofluorimeter with an F2T11 special configuration. Fluorescence lifetime measurements [27] were made on a multiplexed time-correlated single-photon counting fluorimeter (Edinburgh Instruments, model 299T). Fluorescence lifetime in water was measured on a time-correlated single-photon counting system which uses a synchronously pumped cavity dumped, rhodamine 6G dye laser pumped by a mode-locked argon ion laser as an excitation source. Details are given elsewhere [29]. Fluorescence quantum yields were measured using *p*-(dimethylamino)phenyl-3,3-dimethyl-3*H*-indole in methanol as a standard ($\Phi_F = 0.24$) [27].

The temperature variation was achieved with the sample placed in a cell compartment, whose walls were accessible to water circulation. Water from a thermostatted water bath was allowed to circulate through the walls of the sample compartment. The final temperature of the sample was measured by means of a thermocouple immersed in the sample solution and connected to a Fluke 51 digital meter. The scale used for measuring the dielectric constants in methanol–water mixtures was obtained from Harned and Owen [39].

3. Results and discussion

3.1. Nature of the probe solubilization site

Molecule I, was solubilized in SDS and CTAB surfactant micelles and DODAB vesicles. The solubilization of this probe in organized media was ascertained on the basis of spectral shifts, high fluorescence quantum yields and lifetimes compared with those in water. In order to estimate the polarity values and nature of the binding site of this probe in the above-mentioned organized assemblies, the correlations of spectral shifts with different polarity parameters in homogeneous en-

vironment was attempted. No correlation could be made when all solvents of different nature, i.e. non-polar, polar and polar protic were plotted on the same scale. However, separately non-polar or polar protic solvents could be fitted on dielectric functions scales. This is because specific interactions (hydrogen bonding complexes) are taking place between the probe and the protic environments [40]. In other words, the uncomplexed molecule I can serve as a polarity probe in non-polar environments and the complexes can play the same role in environments which are protic such as the microheterogeneous media.

Fig. 1 shows the plot of Stokes shifts (reciprocal centimeters) vs. dielectric constant D for this molecule in alcohols of increasing chain length and methanol–water mixtures. There is an excellent linearity in the plot with a correlation coefficient $r=0.99$. The following linear equation was obtained from the plot of Fig. 1:

$$\bar{\nu}_A - \bar{\nu}_F = 17.69D + 4908 \quad (1)$$

The linearity in Fig. 1 is only obtained because of the double hydrogen bonding that operates only in the ground electronic state of molecule I in the presence of water. When Stokes shifts are plotted against the function $f(D)=(2D-1)/2(D+1)$, the same data could be split into two regions as shown in Fig. 2: a region with low slope, where only alcohols fall, and a higher slope region, which covers methanol–water mixture data. The different slopes in Fig. 2 are due to the fact that water, contrary to the alcohols, is acting as a hydrogen bond donor to the lone pair of the terminal amino group in the ground electronic state of molecule I and also, as in alcohols, a hydrogen bonding interaction takes place at the ring nitrogen atom giving rise to a double hydrogen bonding complex stabilized in the ground electronic state [40]. Contrary to the ground state in water, a single hydrogen bonding complex at

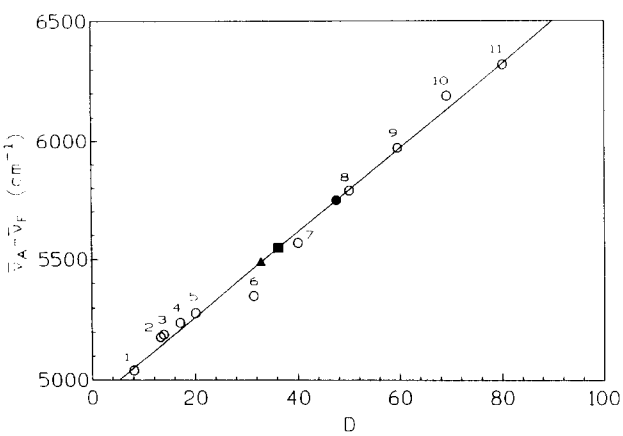

Fig. 1. Stokes shifts of molecule I as a function of the dielectric constant D: 1, n-decanol; 2, n-hexanol; 3, n-pentanol; 4, n-butanol; 5, n-propanol; 6–11, methanol–water mixtures (6, 100:0; 7, 80:20; 8, 60:40; 9, 40:60; 10, 20:80; 11, water); ●, SDS; ■, DODAB; △, CTAB.

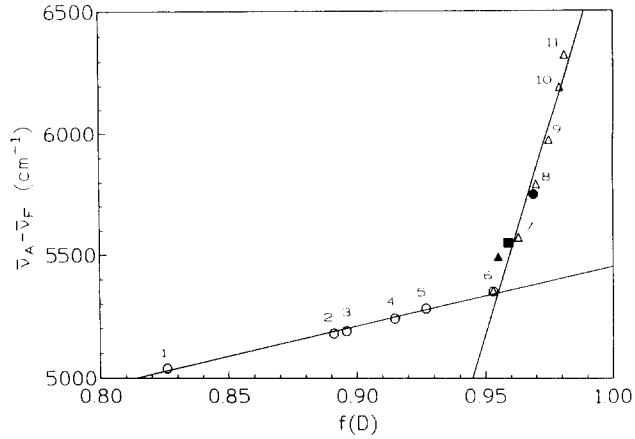

Fig. 2. Stoke shifts of molecule I as a function of $f(D)=(D-1)/(2D+1)$; symbols as for Fig. 1.

Table 1
Spectral characteristics of the neutral species at the center of mass of molecule I and polarity values estimated in various organized media at 298 K

Number	Medium	$\bar{\nu}_A$ (cm^{-1})	$\bar{\nu}_F$ (cm^{-1})	$\bar{\nu}_A-\bar{\nu}_F$ (cm^{-1})	D	$f(D)$
1	Water (pH 9)	26500	20300	6200	80.2	0.981
2	SDS (0.06 M) (pH 10)	26100	20300	5800	48	0.969
3	CTAB (0.01 M) (pH 8)	25800	20300	5500	33	0.955
4	DODAB (0.0028 M) (pH 8)	26100	20500	5600	36	0.959

the ring nitrogen atom is responsible for the stabilization of the relaxed singlet excited state in water and in the alcohols giving rise to two solvatochromic behaviors depending on the presence of water or not.

Spectral characteristics of molecule I in water, SDS, CTAB and DODAB are compiled in Table 1, and the fluorescence spectra of the neutral species in these media are displayed in Fig. 3. It is clear from the figure that the fluorescence spectra are slightly blue-shifted and the Stokes shifts are lower in heterogeneous media compared with water (Table 1). Substituting the values of Stokes shift in Eq. (1) gives polarity values corresponding to a dielectric constant of 48, 33 and 36 for SDS, CTAB and DODAB respectively. The polarity values estimated in organized media are shown graphically in Fig. 1. Considering that the dielectric constant of a typical aliphatic chain compound is 2 and that of water is 80.2, molecule I seems to be located in the interface region of these organized assemblies.

Among these two micelles, the quaternary nitrogen group is more hydrophobic than the sulfate group. Moreover, compared with SDS, CTAB micelles have

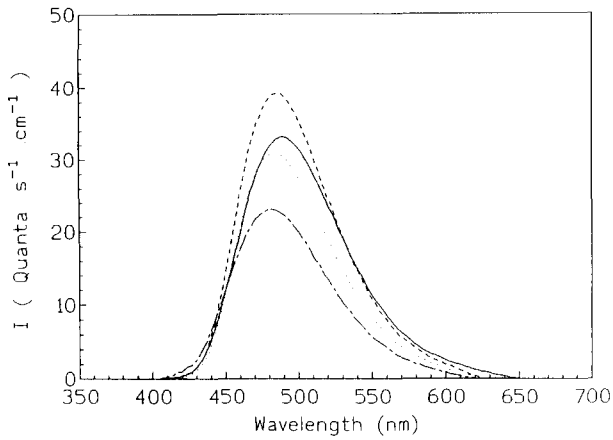

Fig. 3. Fluorescence spectra of molecule I in various media: —, water; ·····, SDS; – – –, CTAB; — — —, DODAB.

larger hydrophobic core and longer alkyl chain (more flexible). This could favor some shift in the mean site of solubilization of molecule I in CTAB somewhat away from the surface toward the hydrophobic core. Since Fig. 2 is able to identify the extent of polarity and hydrogen bonding environment effects on this molecule, the nature of the average binding site in the micelles can be evaluated. The data points for both SDS and CTAB in Fig. 2 show that at the binding site in the micelles, apart from polarity, hydrogen bonding involving water also plays a role. This conclusion is drawn on the basis that if we want to plot the Stoke shift values, on the scale drawn only for alcohols, the points will simulate $f(D)$ values equivalent to which no homogeneous solvent exists. The exposure of molecule I to water molecules is more important in SDS than in CTAB micelles. The polarity values obtained here can be compared with some of the literature values as follows: Zachariasse et al. [17] have determined D values of 51 and 33 for SDS and CTAB respectively using the betaine dye 30 as a polarity probe. Later Drummond et al. [41] using the same probe estimated a value of 56 and 33 for SDS and CTAB respectively based on dioxane–water mixture studies. Kalyanasundaram and Thomas [42] predicted a value of 45 and 16 in SDS and CTAB using pyrene-3-carboxyaldehyde. Law [43] using *p-N,N*-dialkylaminobenzylidene–malononitrile estimated a value of 40 and 36. Mukherjee and Cardinal [44] have reported a similar value of 49 for both SDS and CTAB using benzene as a probe. Kano et al. [19] also estimated qualitatively that the polarity of SDS is higher than CTAB. Similarly, other groups have determined the polarity values in SDS and CTAB [46–49]. It could be generalized from these values that in SDS micelles polarity value ranges from 40 to 55 and for CTAB the polarity values lie around 35. The polarity value reported by Kalyanasundaram and Thomas in CTAB is exceptionally low. This was confirmed to be due to the inappropriate choice of solvents later [45]. Our results also fall within the range of values discussed above. However, it must be mentioned here that the polarity and the nature of environment sensed by an individual molecule depend on its location, its interaction with the medium and the appropriate choice of the solvent series. In spite of these factors, the scatter in the polarity values of SDS micelles is much higher than that for CTAB. This might also be due to the high surface roughness of SDS [18] (see our discussion on photophysical data).

In the case of DODAB vesicles, a temperature variation between 283 K and 343 K was carried out. A detailed discussion on the change in spectral and photophysical parameters of molecule I together with the morphological changes of DODAB vesicles due to temperature changes has been reported by us recently [36]. It was shown that the temperature-dependent spectral shifts are due to changes in polarity and/or hydrogen bonding in the immediate vicinity of the probe. With the increase in temperature, the probe is displaced toward the center of the bilayer, probably with the simultaneous formation of water channels. After the gel to liquid crystalline phase transition, the molecule seems to be in a fixed position. The penetration of water molecules after the phase transition through these channels could have been facilitated leading to higher polarity values sensed by the probe. Another plausible explanation would be that, at higher temperatures, the DODAB vesicles are transformed into micelles [50,51]. We cannot actually discriminate between these two assumptions. This behavior is completely absent in SDS and CTAB. In other words it can be concluded that the vesicle structure is loose and porous and its permeability to external substrates (such as water) is a function of temperature.

The fluorescence band maxima (at the center of mass) of I in alcohols and methanol–water mixtures, at room temperature, have been plotted against D (plot not shown). An excellent linear correlation (with correlation coefficient $r=0.99$) generated the following linear equation:

$$\tilde{\nu}_F = 9.41D + 20\,866 \quad (2)$$

Substituting the $\tilde{\nu}_F$ data obtained in DODAB at various temperatures in Eq. (2), D values were obtained. The dielectric constants D thus estimated in DODAB for molecule I as a function of temperature are plotted in Fig. 4. The D values are higher as usual at low temperatures ($D=47$ at 283 K). D decreases to a minimum at 313 K ($D=26$) and starts increasing again with further increase in temperature. The sudden drop in the D values can be accounted for by the phase transition temperature ($T_c=309$ K) from the gel to the liquid crystalline phase in DODAB. Similar temperature variation was also carried out in water, SDS and CTAB [36]. The fluorescence wavenumber maxima as well as

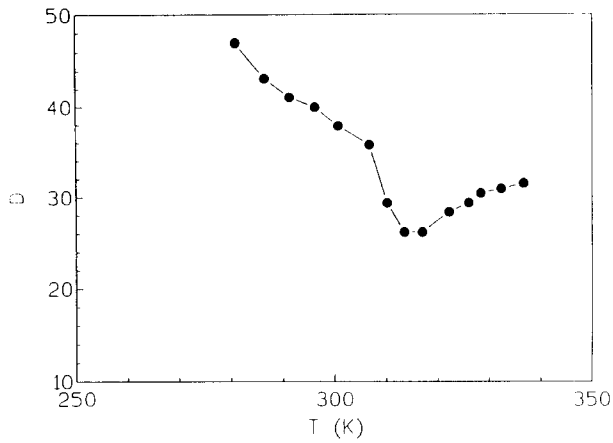

Fig. 4. Variation in the dielectric constant of molecule I in DODAB as a function of temperature.

the bandwidth were found to be independent of the temperature change in micelles. Thus, the thermally induced changes in the spectral parameters of molecule I in DODAB are not due to variations in the solvation of the excited probe. The variation in the D value with temperature can be related to what we just discussed above, that the initial decrease in D is due to the movement of the probe (and the water molecules) toward the center of the bilayer and, after the phase transition, the D values increase as a result of the fixed probe location and subsequent water penetration in the bilayer region or the transformation of the DODAB vesicles into micelles [50,51]. Considering the polarity of the core as equivalent to that of n-heptane or any other non-polar solvent, we should have observed D values equivalent to unity, if the molecule is displaced deep enough into the center or the core of the bilayer. Our lowest polarity value of 26 does not suggest this. That would mean the molecule is deeply buried in the bilayer region, but not deeply enough to be located in the center of the bilayer far away from the head groups. We also admit that the penetration of water molecules is facilitated through the water channels in DODAB formed owing to temperature-dependent morphological changes. However, since the probe location, even before the phase transition, changes constantly with the penetration of water molecules, the new environment occupied by the molecule could never be as hydrophobic as n-heptane. So, even if the molecule reaches the center of the bilayer, it would not be able to detect the hydrophobic environment completely such as any other non-polar solvent. At present it is not possible to differentiate between these two explanations.

The trend in the polarity determined in this work, i.e. SDS > DODAB > CTAB, at 298 K is in accordance with the literature [23,47,48]. However, the polarity value of DODAB can be best compared with that reported by Lukac [24]. Others have used different polarity scales [23,47,48] and some report highly qualitative values of polarity in DODAB [26]. The probe used by Lukac [24] also became displaced toward the center of the bilayer as a function of temperature. The only difference made by our probe is the increase in polarity values after the phase transition of DODAB vesicles, which indicates the formation of water channels and the penetration of water molecules in the bilayer or the transformation of DODAB vesicles into micelles. Lukac reports a polarity value $D=41$ for DODAB, slightly higher than that obtained with our probe ($D=36$) at room temperature. The magnitude of the change in polarity as a function of temperature is about the same (i.e. 20 units) estimated by both probes but our probe is definitely buried deeper at the phase transition than that of Lukac. The dielectric constant determined by both probes is considerably higher than those reported for the phospholipid vesicles [18,24,46]. This leads to the conclusion that, on average, the extent of water penetration in the hydrophobic region of the bilayer is much higher in the case of DODAB than for phospholipids, possibly as a result of the repulsion caused by the charged head groups in the case of cationic DODAB vesicles. The fact that the polarity sensed by our probe is greater after the phase transition of DODAB contradicts the general belief of exclusion of water out of the bilayer region after the gel to liquid phase transition in vesicles [24]. The expulsion of our probe out of the bilayers after the phase transition can be ruled out on the basis that the fluorescence quantum yield of molecule I increases during the phase transition of DODAB and the activation energy E_a of the decay processes is higher (11.8 kJ mol^{-1}) after the phase transition than before (5.7 kJ mol^{-1}) [36]. These facts strongly support the argument that the molecule resides in a less polar protic, more viscous region of the bilayer after the phase transition of DODAB.

3.2. Photophysics

Table 2 summarizes all the photophysical parameters determined for this molecule in different homogeneous and microheterogeneous media. Data show that various quantities are sensitive to viscosity and polarity of the environment. The origin of these effects on photophysical parameters is as follows. Conformational analysis of this molecule using AMPAC and INDO-S calculations has predicted that the phenylic moiety possesses a certain degree of torsional freedom which is considered to be the main pathway for the radiationless processes in non-polar media. The torsional movement is greatly affected by viscosity and polarity and/or proton donor capacity of the solvent [29,40]. Therefore the Φ_F and τ_F values in Table 2 increase in going from n-heptane to n-hexanol with a corresponding decrease in k_{nr} values. However, in the case of water, the larger increase in k_{nr} has been proposed to be due to the

Table 2
Photophysical parameters of molecule I in various media at 298 K

Number	Medium	Φ_F	τ_F (ns)	$k_F \times 10^{-8}$ (s^{-1})	$k_{nr} \times 10^{-8}$ (s^{-1})
1	*n*-heptane	0.072	0.19	3.8	49
2	*n*-hexadecane	0.27	0.59	4.6	12
3	Acetonitrile	0.31	1.94	1.6	3.6
4	Methanol	0.25	1.8	1.4	4.2
5	*n*-hexanol	0.28	2.01	1.4	3.6
6	Water (pH 9)	0.013	0.073 [a]	1.8	137
7	SDS (0.06 M) (pH 10)	0.13	1.5 [b]	0.9	6.0
8	CTAB (0.01 M) (pH 8)	0.24	1.9	1.3	5.4
9	DODAB (0.0028 M) (pH 8)	0.22	2.2	1.0	4.5

[a] Main component of a triexponential decay curve [39].
[b] $\langle\tau\rangle = \sum_i a_i\tau_i^2 / \sum_i a_i\tau_i$ (see text for the details of the two components).

population of a low energy non-emissive TICT state [31,40] which might also depend on the viscosity and polarity of the environment.

An increase in the Φ_F and τ_F values and a decrease in k_{nr} is observed in micelles and vesicle media. Even if this increase plays against any kind of external quenching, the possibility of quenching of the probe fluorescence by bromide counterions in CTAB and DODAB is ruled out on the basis that bromide ions do not quench the fluorescence of the molecule in pure aqueous medium. Additionally, quantum yields for the probe molecule were checked at various concentrations of CTAB and found to increase with increase in micelle concentration. We have discussed in the last section that molecule I in micelles and vesicles is located in an environment in water although influenced by hydrogen bonding. Since there is no obvious correlation of the viscosity of the solvent with the photophysical constants of molecule I [29] in the case of polar protic solvents, the estimation of quantitative values of viscosity at the binding site of SDS, CTAB and DODAB is impossible. However, high values of Φ_F, τ_F and low values of k_{nr} in micelles and vesicles compared with water at 298 K suggest that the molecule occupies a fairly high viscous, polar protic environment in these organized assemblies where population of the TICT state is inhibited. Among SDS, CTAB and DODAB, the latter seems to exhibit the lowest k_{nr} values even though these variations are inside the experimental error. On the contrary, the polarity values indicate that the molecule occupies a slightly higher polar protic environment in DODAB compared with CTAB.

The fluorescence decay analysis shows that the decay curves for molecule I are singly exponential in CTAB and DODAB. In the case of SDS, the single-exponential fitting function gave bad statistics ($\chi^2 = 1.61$; DW = 1.37). However, on trying a double-exponential fitting function, the statistics greatly improved ($\chi^2 = 1.04$; DW = 1.95) and no further improvement could be obtained using higher exponential fitting functions (Fig. 5). The major component with a pre-exponential factor equal to 0.8 has a shorter lifetime ($\tau_F = 1.3$ ns) than the minor component (pre-exponential factor equal to 0.2, $\tau_F = 2.0$ ns). Single fluorescence lifetime in CTAB and DODAB indicates that molecule I is solubilized at only one solubilization site in these organized media. The two lifetimes in SDS suggest a fractional distribution of the molecules at two different sites of SDS having different polarities and viscosities. Since molecule I at the binding site of SDS micelles probes a dielectric constant close to those obtained for the 60:40 and 40:60 methanol–water mixtures (Fig. 2), the fluorescence decay curves have also been obtained in these two mixtures. Results show that the decay curve in the 60:40 methanol–water mixture can be fitted with a single-exponential function ($\tau_F = 0.89$ ns) whereas the lifetime obtained for the 40:60 methanol–water mixtures is described more accurately by a double-exponential decay function ($A_1 = 0.98$, $\tau_1 = 0.46$ ns; $A_2 = 0.02$, $\tau_2 = 1.2$ ns). However, the second component of the double-exponential function is as weak as that of the fluorescence decay curve of I observed in pure water [40]. Thus mainly one conformer or complex is responsible for the fluorescence of I observed in polar protic homogeneous media.

The results could be discussed on the basis of morphologies of micelles. Menger and Doll have proposed the structure of small micelles to be rough owing to the looping of hydrophobic chains [52,53]. These irregularities caused by the surface roughness are filled by water molecules. Support for this has also been provided by other researchers using small angle neutron scattering data [54,55]. However, similar roughness on the surface of CTAB micelles is absent [54,56]. It thus seems that the surface of SDS micelles offers two different solubilization sites to two distinct conformers or complexes. In other words, molecule I seems to be able to recognize two different sites in SDS micelles. In order to know more about this, the reader is referred to a recent paper [35] where the behavior of this molecule has been compared with four other substituted 3*H*-indole derivatives. Since DODAB vesicles give rise to monoexponential decay, the surface morphology of these vesicles can be considered as smooth as in CTAB micelles. This argument for DODAB vesicles also holds good on the basis of the Menger model, which predicts surface roughness only for small sized microstructures such as SDS micelles [52,53].

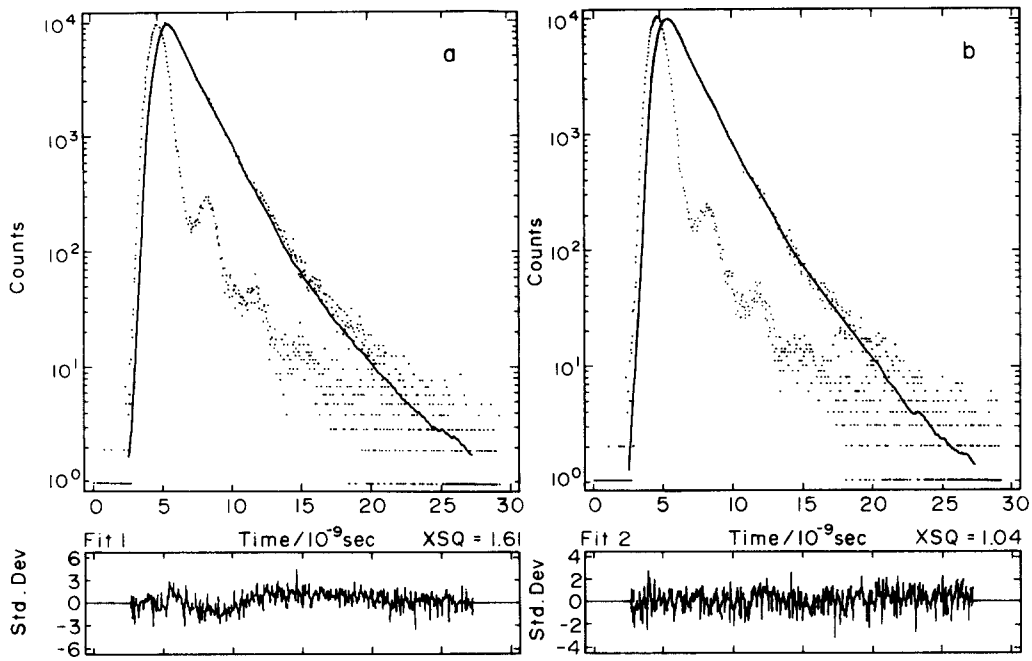

Fig. 5. Fluorescence decay curve of molecule I in SDS: (a) single-exponential fit; (b) double-exponential fit.

3.3. pH effects

Our recent pH studies on this molecule [31,40] and other substituted derivatives of 3*H*-indole in aqueous medium have shown that the first preferred protonation site among other available basic centers is the tertiary ring nitrogen atom. In the absorption spectrum, on decreasing pH from 9 to 2, a largely red-shifted, highly intense and structured band corresponding to the monocation was observed at the expense of the neutral species. On the contrary, the fluorescence spectrum of the monocation species was also highly structured but slightly red shifted and the fluorescence intensity was quenched by approximately an order of magnitude compared with the neutral species. INDO-S semiempirical calculations have shown that non-emissive low energy TICT state formation might be responsible for the drastic fluorescence quenching of the monocation species [31]. The ground state pK_a value of the neutral–monocation equilibrium was determined to be 4.8.

Table 3
Absorption spectral characteristics of neutral and monocation species at peak maxima of molecule I in water and organized media at 298 K

Number	Medium	Species	$\bar{\nu}_A$ (cm^{-1})	ϵ (M^{-1} cm^{-1})	R
	Water	Neutral (pH 9)	26500	30200	
		Monocation (pH 2)	23100 22100	59900 66700	1.98 2.21
	SDS (0.06 M)	Neutral (pH 10)	26000	30600	
		Monocation (pH 3)	22900 21800	50000 64000	1.67 2.06
	CTAB (0.01 M)	Neutral (pH 8)	25600	30000	
		Monocation (pH 1.0)	23100 22200	45300 49300	1.51 1.64
	DODAB (0.0028 M)	neutral (pH 8)	26300	–	
		Monocation (pH 1.5)	23300 22200	– –	1.58 1.58

In order to see the effect of micelles and vesicles on neutral–monocation equilibrium, similar studies of pH effects were carried out in the pH range 10–1 in these media. The relevant data are compiled in Table 3. The absorption spectra of neutral and monocation species in water, SDS, CTAB and DODAB are displayed in Fig. 6. Considering for example CTAB, the following differences compared with the aqueous medium are noted.

(1) The appearance of the monocation band starts at much lower pH (below 4) [31].
(2) The absorbance of the monocation becomes constant at pH ≈ 1 and does not change any further with a slight decrease in pH [31].
(3) The molar extinction coefficient ϵ for the peak maxima of the monocation is lower. Thus the ratio R of intensity of the monocation band to the neutral band becomes significantly smaller (see Table 3).
(4) The bandwidth of the monocation in CTAB is larger (2900 cm^{-1}) than that in an aqueous medium (2600 cm^{-1}).

CTAB micelles are positively charged and hence should destabilize any types of cationic species on the surface. They do exhibit some affinity for protons as

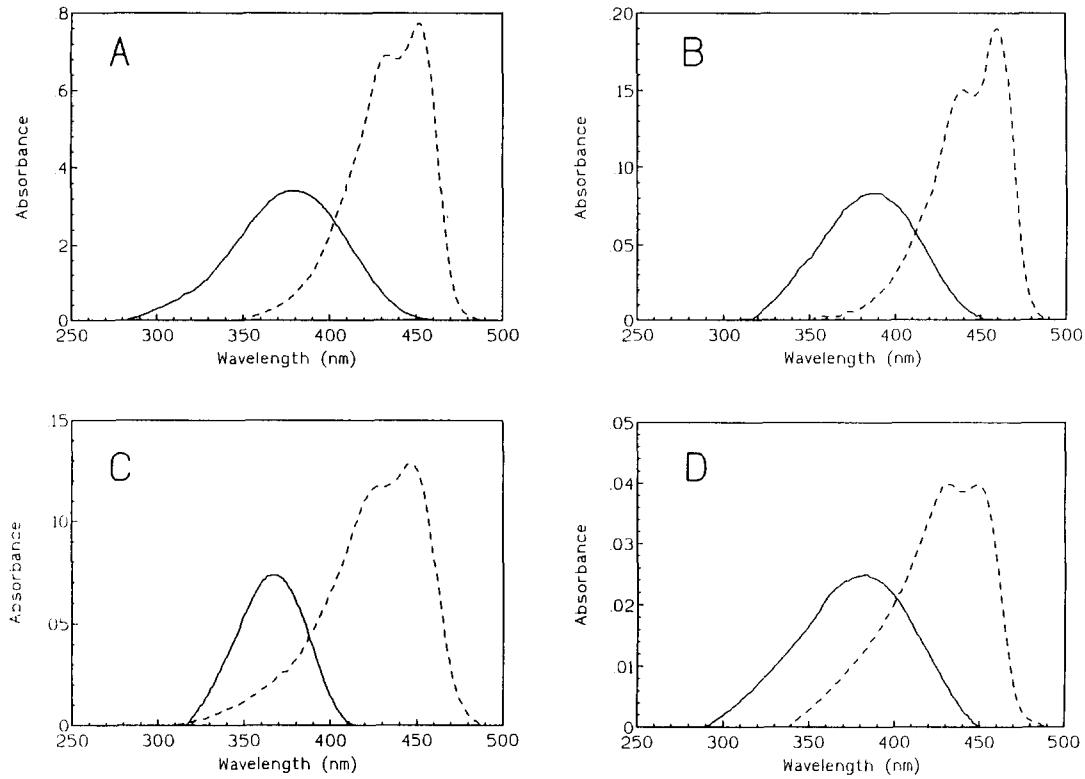

Fig. 6. Absorption spectra of neutral (——) and monocation (– – –) species of molecule I in various media: (a) in water; (b) in SDS; (c) in CTAB; (d) in DODAB.

is clear from the existence of the neutral–monocation equilibrium, although low pH is required compared with aqueous medium. Since the absorbance of the monocation is low and the bandwidth is high in the presence of CTAB, it can be safely concluded that the complete conversion of neutral to monocation has not taken place. It is probably due to the saturation of proton accepting sites at the interface of CTAB. In order to see the surface saturation effect, anionic micelle SDS was selected because it should be highly receptive to protons and at much higher concentrations. The choice was thought to be the more appropriate because, apart from being anionic, it provides two different sites to molecule I, as revealed by the fluorescence lifetime decay analysis. The pH study between 10 and 1 was undertaken. The appearance of the monocation band in the absorption spectrum started at a much higher pH compared with water and CTAB and the whole reaction was completed at pH 3.5. The appearance of nearly similar ϵ values, similar absorbance ratio of the monocation to neutral band, and the similar bandwidth (2500 cm^{-1}) as observed in water suggest that the conversion to monocation species is complete in SDS. Similar effects were observed in the fluorescence spectra. The ground state pK_a value for the neutral–monocation equilibrium is 6.8 and is higher than in water (4.8) [31] and what would have been observed in CTAB, if the protonation reaction would have been completed. The pH effects in DODAB followed a behavior similar to that of CTAB, and the ratio of the monocation to the neutral absorbance was nearly similar to that of CTAB. The effect of micelles and vesicles on the protonation equilibrium of molecule I can be explained on the basis of the pseudophase ion exchange model [57]. In terms of this model, the shift in pK_a values is caused by the transfer of molecule I and the protons from the aqueous phase into a much smaller volume of the micellar pseudophase. Since SDS micelles stabilize both forms of molecule I (i.e. neutral and monocation) and the protons, an increase in the pK_a value is observed compared with water. On the contrary, the cationic surfaces of CTAB and DODAB repel protons and the monocations of molecule I and a lowering in the pK_a values is expected. Similar effects of organized media on equilibrium reactions have also been observed recently [58–60].

4. Concluding remarks

Spectral correlations or probe I with the polarity parameters in alcohols and methanol–water mixtures have allowed us to determine the polarity and nature of the binding site in the organized assemblies used. Values corresponding to dielectric constant $D = 48$, 33 and 36 for SDS, CTAB and DODAB respectively have

been estimated and agree reasonably well with the literature values. It has been further evidence that, in addition to polarity, hydrogen bonding also plays a role at the binding site. Spectral variation with change in temperature in DODAB shows that the probe migrates toward the center of the bilayer, far away from the head groups of DODAB. The D values vary between 47 and 26 in this temperature range. The observed increase in polarity values at temperatures higher than the phase transition temperature might be ascribed to a fixed location of the probe and penetration of water molecules toward the binding site of molecule I in DODAB or to the transition of DODAB vesicles into micelles. The first explanation would contradict the general belief of expulsion of water molecules out of the bilayers at higher temperatures. Fluorescence decay time analysis has shown that the probe recognizes only one site in CTAB and DODAB, whereas it exhibits a double site occupancy in SDS micelles. The lowest value of k_{nr} in DODAB suggests the site to be highly viscous although more polar compared with CTAB. Effect of micelles and vesicles on the neutral–monocation protonation equilibrium shows that the extent of formation of the monocation as a function of the pH depends on the surface charge type, being less favored on the cationic surfaces than on the anionic. These micelles and vesicular effects on protonation equilibrium can be rationalized by the pseudophase ion exchange model.

Acknowledgments

The financial assistance of the Natural Science and Engineering Research Council of Canada and the "Fonds FCAR" (Québec) is gratefully acknowledged. We would also like to thank Mr. Adrian Popowycz for the synthesis and purification of molecule I studied here and Dr. Shalini Nigam of our laboratory for the study of bromide ions effect on the fluorescence of the probe.

References

[1] J.H. Fendler, *Membrane Mimetic Chemistry,* Wiley Interscience, New York, 1982.
[2] M. Gratzel and K. Kalyanasundaram (eds.), *Kinetics and Catalysis in Microheterogeneous Systems,* Surfactant Science Series, Vol. 38, Dekker, New York, 1991.
[3] J.L. Thomas and D.A. Tirrell, *Acc. Chem. Res., 25* (1992) 236.
[4] A.K. Lala and E.R. Kumar, *J. Am. Chem. Soc., 115* (1993) 3982.
[5] J.K. Thomas, *Chem. Rev., 180* (1980) 283.
[6] N.J. Turro, M. Gratzel and A.M. Braun, *Angew Chem., Int. Edn. Engl., 19* (1980) 675.
[7] J.H. Fendler, *Acc. Chem. Res., 13* (1980) 7.
[8] T. Kunitake and Y. Okahata, *J. Am. Chem. Soc., 99* (1977) 3860.
[9] A.M. Carmona-Ribeiro, *Chem. Soc. Rev., 21* (1992) 209.
[10] J.N. Robinson, D.J. Cole-Hamilton, M.K. Whittlesey and P. Camilleri, *J. Chem. Soc., Faraday Trans., 86* (1990) 2897.
[11] G. Gregoriadis, *Nature (London), 265* (1977) 407.
[12] P.J. Pratt, Y.S. Kang and L. Kevan, *J. Phys. Chem., 96* (1992) 5629.
[13] C.A. Bunton, F. Nome, F.H. Qnina and L.S. Romsted, *Acc. Chem. Res., 24* (1991) 357.
[14] S. Nigam, R.S. Sarpal and S.K. Dogra, *J. Colloid Interface Sci., 163* (1994) 152.
[15] V. Ramamurthy (ed.), *Photochemistry in Organized and Constrained Media,* VCH, New York, 1991.
[16] J.S. Nowick, J.S. Chen and G. Noronha, *J. Am. Chem. Soc., 115* (1993) 7636.
[17] K.A. Zachariasse, N.V. Phuc and B. Kozankiewicz, *J. Phys. Chem., 85* (1981) 2676.
[18] F. Grieser and C.J. Drummond, *J. Phys. Chem., 92* (1988) 5580.
[19] K. Kano, Y. Veno and S. Hashimoto, *J. Phys. Chem., 81* (1985) 3161.
[20] P. Mukherjee and J. Ko, *J. Phys. Chem., 96* (1992) 6090.
[21] C. Gamboa and A.F. Olea, *Langmuir, 9* (1993) 2066.
[22] E. Pérochon, A. Lopez and J.F. Tocanne, *Biochemistry, 31* (1992) 7672.
[23] D.R. Suddaby, P.E. Brown, J.C. Russell and D.J. Whitten, *J. Am. Chem. Soc., 107* (1985) 5609.
[24] S. Lukac, *J. Am. Chem. Soc., 106* (1984) 4386.
[25] A. Safarzadeh-Amiri, M. Thompson and V.J. Krull, *J. Photochem. Photobiol. A: Chem., 49* (1989) 151.
[26] B.C.R. Guillaume, D. Yogev and J.H. Fendler, *J. Phys. Chem., 55* (1991) 7489.
[27] M. Belletête and G. Durocher, *J. Phys. Chem., 93* (1989) 1793.
[28] M. LaChapelle, M. Delletête, M. Poulin, N. Godbout, F. LeGrand, A. Héroux, F. Brisse and G. Durocher, *J. Phys. Chem., 25* (1991) 9764.
[29] M. Belletête and G. Durocher, *J. Phys. Chem., 96* (1992) 9183.
[30] M. Belletête, R.S. Sarpal and G. Durocher, *Chem. Phys. Lett., 201* (1993) 145.
[31] R.S. Sarpal, M. Belletête and G. Durocher, *Can. J. Chem., 71* (1993) 1570.
[32] J.R. Lakowicz, P.A. Koen, H. Szacinski, I. Gryczynski and J. Kusban, *J. Fluoresc., 4* (1994) 117.
[33] M. Belletête, M. LaChapelle and G. Durocher, *J. Phys. Chem., 91* (1990) 5337, 7642.
[34] R.S. Sarpal, M. Belletête and G. Durocher, *J. Phys. Chem., 97* (1993) 5007.
[35] R.S. Sarpal, M. Belletête and G. Durocher, *Chem. Phys. Lett., 221* (1994) 1.
[36] R.S. Sarpal and G. Durocher, *J. Photochem. Photobiol. A: Chem., 80* (1994) 307.
[37] P. Skrabal, J. Steiger and H. Zellinger, *Helv. Chim. Acta, 58* (1975) 800.
[38] A. Popowycz, *M.Sc. Thesis,* Université de Montréal, 1992.
[39] H.S. Harned and B.B. Owen, *The Physical Chemistry of Electrolytic Solutions,* Reinhold, New York, 3rd edn., 1958, p. 161.
[40] M. Belletête, R.S. Sarpal and G. Durocher, *Can. J. Chem., 72* (1994) 2239.
[41] C.J. Drummond, F. Grieser and T.W. Healy, *Faraday Discuss. Chem. Soc., 81* (1986) 95.
[42] K. Kalyanasundaram and J.K. Thomas, *J. Phys. Chem., 81* (1977) 2176.
[43] K.Y. Law, *Photochem. Photobiol., 33* (1981) 799.
[44] P. Mukherjee and J. Cardinal, *J. Phys. Chem., 82* (1978) 1620.
[45] J.C. Dederen, L. Coosemens, F.C. DeSchryver and A. Van Dormael, *Photochem. Photobiol., 30* (1979) 443.

[46] K.S. Schanze, D.M. Shin and D.G. Whitten, *J. Am. Chem. Soc., 107* (1985) 507.
[47] K.S. Schanze, T.F. Malton and D.G. Whitten, *J. Am. Chem. Soc., 104* (1982) 1733.
[48] D.M. Shin, K.S. Schanze, J.P. Otruba, P.E. Brown and D.G. Whitten, *Isr. J. Chem., 28* (1987) 37.
[49] T. Handa, K. Matsuzaki and M. Nakagaki, *J. Colloid. Interface Sci., 116* (1987) 50.
[50] D.D. Miller and D.F. Evans, *J. Phys. Chem., 93* (1989) 323.
[51] D.D. Miller, L.J. Magid and D.F. Evans, *J. Phys. Chem., 94* (1990) 5921.
[52] F.M. Menger and D.W. Doll, *J. Am. Chem. Soc., 106* (1984) 1109.
[53] F.M. Menger, *Angew Chem., Int. Edn. Engl., 30* (1991) 1086.
[54] J.B. Hayter and J. Penfold, *Colloid Polym. Sci., 261* (1983) 1022.
[55] R. Triolo, E. Caponetti and V. Graziano, *J. Phys. Chem., 89* (1985) 5743.
[56] S.S. Berr, E. Caponetti, J.S. Johnson, R.M. Jones and L.J. Magid, *J. Phys. Chem., 90* (1986) 5766.
[57] L.S. Romsted and D. Zanette, *J. Phys. Chem., 92* (1988) 4690.
[58] S. Lukac, *J. Phys. Chem., 87* (1983) 5045.
[59] R.S. Sarpal and S.K. Dogra, *J. Photochem. Photobiol. A: Chem., 69* (1993) 329.
[60] Y.V. Il'ichev, A.B. Demyashkevich, M.G. Kuzmia and H. Lemmetyinen, *J. Photochem. Photobiol. A: Chem., 74* (1993) 51.